Indentation Plastometry for Study of Anisotropy and Inhomogeneity in Maraging Steel Produced by Laser Powder Bed Fusion

Tom Southern, Jimmy E. Campbell, Kyriakos I. Kourousis, Barry Mooney, Yuanbo T. Tang, and Trevor William Clyne*

This work concerns the use of profilometry-based indentation plastometry (PIP) to obtain mechanical property information for maraging steel samples produced via an additive manufacturing route (laser powder bed fusion). Bars are produced in both "horizontal" (all material close to the build plate) and "vertical" (progressively increasing distance from the build plate) configurations. Samples are mechanically tested in both as-built and age-hardened conditions. Stress–strain curves from uniaxial testing (tensile and compressive) are compared with those from PIP testing. Tensile test data suggest significant anisotropy, with the horizontal direction harder than the vertical direction. However, systematic compressive tests, allowing curves to be obtained for both build and transverse directions in various locations, indicate that there is no anisotropy anywhere in these materials. This is consistent with electron backscattered diffraction results, indicating that there is no significant texture in these materials. It is also consistent with the outcomes of PIP testing, which can detect anisotropy with high sensitivity. Furthermore, both PIP testing and compression testing results indicate that the changing growth conditions at different distances from the build plate can lead to strength variations. It seems likely that what has previously been interpreted as anisotropy in the tensile response is in fact due to inhomogeneity of this type.

1. Introduction

Maraging steels are among the alloy types of particular interest in the context of additive manufacturing (AM), partly because they present certain difficulties during production of components with complex geometries via conventional routes. These steels contain high levels of Ni ($\approx$15–25 wt%), intermediate levels of secondary alloying elements (such as Co, Mo, and Ti), and very low levels of carbon ($<\approx$0.03 wt%). Stainless versions are also available, with moderate levels of Cr. High strengths are developed during heat treatments via the formation of fine intermetallic constituents. A typical treatment would comprise a short period of austenitizing at $\approx$800–1000 °C, cooling to room temperature (forming a Fe–Ni martensitic phase, with relatively good ductility), and then aging at $\approx$500 °C to produce a fine dispersion of intermetallics (such as Ni_3Ti) along dislocations left by the martensite formation. Common grade designations, such as 200, 250, 300, etc., refer to approximate tensile strengths expressed in ksi. They thus have high strengths (between about 1.4 and 2.4 GPa), combined with good toughness, machinability (before heat treatment), and durability at relatively high temperature (up to $\approx$400 °C). Applications include several highly demanding ones in aerospace, such as landing gear, helicopter undercarriages, etc. In view of the sensitivity of these alloys to the details of the heat treatment and associated microstructural changes, development work is needed to optimize the properties when using AM production routes.

The main AM methodologies applied to this class of material are wire arc additive manufacturing (WAAM) and laser powder bed fusion (LPBF). In both cases, there is potential concern about the presence of porosity, with reported levels varying over quite a

---

T. Southern, J. E. Campbell, T. W. Clyne
Plastometrex Ltd.
204 Science Park, Milton Road, Cambridge CB4 0GZ, UK
E-mail: twc10@cam.ac.uk

K. I. Kourousis, B. Mooney
School of Engineering
University of Limerick
V96 TPX Limerick, Ireland

K. I. Kourousis
CONFIRM Smart Manufacturing Research Centre
Unit 2, Park Point, Dublin Road, Castletroy, V94 C928 Limerick, Ireland

Y. T. Tang
Department of Materials
21 Banbury Rd., Oxford OX2 6HT, UK

T. W. Clyne
Department of Materials Science
27 Charles Babbage Road, Cambridge CB3 0FS, UK

**ADVANCED
SCIENCE NEWS**

www.advancedsciencenews.com

**steel
research**
international

www.steel-research.de

wide range. The advantages of WAAM, as applied to maraging steels,[1–3] largely relate to higher production rates, but the structure and surface finish tend to be relatively coarse, and the porosity level can be high. In general, the LPBF technique has been more popular than WAAM for maraging steels,[4–10] offering superior scope for geometrical and microstructural control.

A major difficulty in assessing the mechanical characteristics of AM components is associated with point-to-point property variations in properties, caused by evolution in the growth conditions. These can arise during virtually all types of AM, often over relatively small distances. Most attempts to study these variations have been based on conventional tensile testing and/or hardness measurement. The former is severely handicapped by an inherently limited spatial resolution (plus difficulties in machining of suitable specimens), while hardness numbers are just semiquantitative indicators of the resistance to plastic deformation. Using them in any quantitative way is inadvisable. The spatial precision of uniaxial testing can often be improved by switching to compression, but this does introduce some uncertainty in terms of the effect of friction[11] between sample and platen and in general it is not widely used.

In addition to these difficulties in studying inhomogeneities on a local scale, complications can arise from the mechanical response being anisotropic. This also is not uncommon in AM material and indeed it has been reported many times, often with information about associated texture.[12–15] Referring specifically to LPBF of maraging steels, several recent studies[5,9,16–18] have reported anisotropy, while just a few others[4] have indicated the presence of inhomogeneities (along the growth direction). In view of the inherent limitations of using conventional mechanical testing procedures to detect such effects in AM products, these reports may not be entirely reliable (although there is no doubt that either or both effects can be present in AM components).

There have been several very recent studies of anisotropy from a microstructural point of view. Tian et al.[19] detected no significant texture in LPBF M789 steel, suggesting that anisotropy would be unlikely. On the other hand, Kannan and Nandwana[20] found that, while martensite was untextured, the retained austenite did exhibit texture, potentially leading to at least some anisotropy in the final product. Zhao et al.[17] also reported texture in LPBF 18Ni-300 steel, in combination with different yield strengths in different directions (relative to the build direction), although these differences were in fact relatively small (<10%). The more detailed microstructural study of Paul et al.,[21] also on LPBF 18Ni–300 steel, indicated that solution treatment tended to remove much of the substructure associated with the AM process (such as cellular features and melt pool boundaries), degrading the toughness. However, this could be improved by thermal cycling. Overall, the anisotropy was reported to be low, both microstructurally and from mechanical testing. It may also be noted that a distinction could be drawn between mechanical anisotropy in terms of plasticity—probably mainly due to texture—and in terms of damage development/ cracking, potentially arising from defects in interlayer regions. The study of Dehgahi et al.[22] is also focused on microstructure, particularly the effects of heat treatment, with some (weak) texture detected. Overall, microstructural development aspects clearly involve several potential complications. There have been very few systematic studies of microstructural inhomogeneity on a relatively coarse scale, for example, with distance along the growth direction.

While conventional mechanical testing procedures have limitations for study of AM components, the recently developed methodology of profilometry-based indentation plastometry (PIP) offers important advantages. The procedure involves iterative finite element method (FEM) simulation of the indentation process, with the plasticity parameters (in a constitutive law) being repeatedly changed until optimal agreement is reached between experimental and predicted indent profiles. The Voce law has been found to be effective in capturing the (true) stress–strain relationship exhibited by a wide range of metals. Details are available in a recent paper[23] that reviews various aspects of the PIP methodology. Once this relationship has been established, the behavior in a range of loading configurations, including that of uniaxial tensile testing, can be obtained.

The spatial resolution of the technique is of the order of 1 mm, with minimal sample preparation requirements. It therefore offers a combination of the convenience and spatial resolution of hardness testing with the meaningful outcome of a tensile test. A recent review[23] covers the main issues involved in optimization of experimental and data processing procedures. Integrated facilities are now available that allow stress–strain curves to be obtained automatically from a single-indentation experiment within a timescale of a few minutes. There has also been detailed treatment of sample-specific issues, including the effects of residual stresses,[24] of samples being exceptionally hard,[11] of property variations in and around fusion welds,[25] and of effects such as local inhomogeneities in particulate metal matrix composites.[26] Furthermore, one study[27] was focused on the detection and characterization of anisotropy (in a superalloy component produced via an AM technique). The PIP technique has a high sensitivity for the detection of anisotropy, which clearly has potential value for work in this area.

It has sometimes been claimed that "nanoindenters" can be used to obtain stress–strain relationships, with fine-scale resolution. However, a key finding from a detailed study over recent years[23] is that the plastically deformed volume must be large enough for its mechanical response to be representative of the bulk. This usually requires it to be a "many-grained" assembly, which typically translates into a need for the indenter radius to be of the order of 0.5–1 mm and the load capability to extend to the kN range. This means that nanoindenters (typically having maximum loads of a few tens of Newtons at most) are completely unsuitable.

The current work involves using the PIP methodology to investigate anisotropy and inhomogeneity in LPBF samples made of a particular maraging steel, illustrating the capabilities of the technique in terms of both point-to-point mapping of properties (stress-strain curves) and its sensitivity for the detection of anisotropy.

2. Experimental Section

2.1. Materials and Test Samples

The alloy used is commonly designated MS300, with the "300" indicating a "strength" of about 300 ksi ($\approx$2 GPa). In fact, the

yield stress and ultimate tensile stress (UTS) change substantially during heat treatment and the material is only likely to exhibit strengths of this order after a suitable ageing treatment. The steel powder (18.1% Ni, 8.9% Co, 5.7% Mo, 0.9% Ti) was produced by gas atomization, giving a median size of about 35 µm and no particles above about 50 µm. Test specimens were manufactured using the EOS EOSINT M280 system under a nitrogen atmosphere, with a 200 W Yb-fiber laser. The laser scan strategy involved deposition of layers about 40 µm-thick during each pass, with periodic deposition "stripes" about 300–600 µm in length, spaced about 100 µm apart laterally. The scan direction was rotated by 67° between passes. This created fully dense material, with a complex cellular/dendritic microstructure. The flowability of the (fine, spherical) powder facilitated the elimination of porosity. This rotation angle did not lead to any superimposition of scan directions, even after large numbers of passes, so the resultant material was expected to be transversely isotropic, with the principal axes being the "build" direction (z) and any "transverse" direction (x or y) and no distinction expected between any transverse directions. Full details concerning the processing conditions and microstructure are provided in previous papers.[5,16] The configuration, including the locations and orientations of uniaxial test samples, is depicted in **Figure 1**. Samples were examined in the "as-built" and "age-hardened" state. The latter was after a heat treatment of 12 h at 460 °C, although previous

work[5] indicated that the (tensile) properties were very similar after various heat treatments of this type.

2.2. Microstructural Examination

Optical microscopy was used to examine the free surfaces of regions that had been indented. This was done on a relatively coarse scale, often providing information about both the grain structure and the way in which deformation had taken place in the pile-up region.

Microstructures were also examined at higher magnification, using scanning electron microscopy (SEM), after preparation by grinding and polishing to 3 µm finish. A Zeiss Merlin field-emission gun–scanning electron microscope (FEG-SEM) was used. A Bruker eFlash high-resolution electron backscattered diffraction (EBSD) detector was utilized for acquiring the evolution of crystal orientations. The specimens were subsequently scanned in the SEM at 15 kV electron beam energy, with a probe current of 20 nA. The Kikuchi diffraction patterns were acquired at 160×120 resolution at two magnifications, with a step size of between 440 nm and 1.1 µm, respectively. A low-magnification (200X) map was used for texture interpretation. The diffraction data were analyzed using ESPRIT 2.3 and HKL Channel 5 software. The martensitic phase predominated and this was indexed as if it were just ferrite (bcc).

2.3. Uniaxial Testing

The gauge length of the tensile samples was 32 mm, with a square section of side 6 mm. Details are available in the previous papers.[5,16] Attention is focused here on material in "as-built" and "age-hardened" (12 h @ 460 °C) conditions. Samples for tensile testing were produced in both "horizontal" and "vertical" configurations. For the former, the tested material all came from within about 15 mm of the build plate, whereas for the latter it was from distances between about 70 and 100 mm from the build plate. (This arrangement was adopted in view of the practical difficulties associated with creating samples for testing in the "horizontal" direction at large distances from the build plate.) "Horizontal" samples were thus being tensile tested in a "transverse" (x) direction, whereas "vertical" samples were being tensile tested in the "build" (z) direction. Compression testing was also carried out, on samples machined from the (undeformed) ends of these tensile test pieces. These were oriented either parallel or normal to the tensile axis, so that this testing was done in both "build" and "transverse" directions in each case, see Figure 1. These samples were from material located at about 5–10 mm from the build plate when derived from the "horizontal" tensile sample, and at about 100 and 110 mm from the build plate for those derived from the "vertical" tensile sample.

Compression testing was done using an Instron 3369 loading frame, with a 50 kN capacity. Samples were in the form of cylinders (4 mm diameter and 4 mm long). No lubricant was used. Displacement was measured using a linear variable displacement transducer (LVDT), attached to the upper platen and actuated against the lower one. In addition, Techni-Measure 1 mm linear strain gauges were attached to both sides of each sample. They had a range of up to about 2%. The average value from these
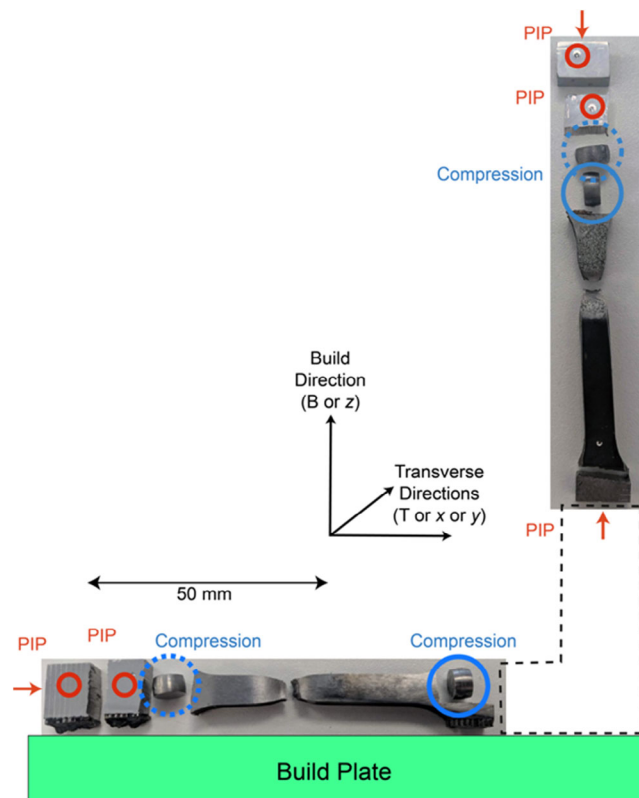
Figure 1. Schematic representation of the build configuration, with photos of the tensile test samples (in "horizontal" and "vertical" orientations). Also indicated are the locations and orientations of the compression and PIP samples machined from the grip sections after these tests.

2200881 (3 of 10)
© 2023 The Authors. Steel Research International published by Wiley-VCH GmbH

ADVANCED
SCIENCE NEWS
www.advancedsciencenews.com

steel
research
international

www.steel-research.de

two was used to apply a compliance correction to the LVDT data. This also removed the uncertainty associated with the "bedding down" effect. Compression testing was carried out in both "build" (z) and "transverse" (x) directions, on samples cut from the grip sections of the tensile samples, these remained elastic during the tensile testing. The locations and orientations of these compression test pieces are shown in Figure 1.

2.4. Indentation Plastometry

The steps involved in a standard PIP operation were 1) pushing a hard spherical indenter into the sample with a known force; 2) measuring the (radially symmetric) profile of the indent; 3) iterative FEM simulation of the test to obtain the set of (V_{oce}) plasticity parameter values giving optimal agreement between measured and modelled profile; and 4) converting the resultant (true) stress–strain relationship to a nominal stress–strain curve that would be obtained during uniaxial testing. Full details are provided in a recent review paper.[23]

Indentation was carried out in both build (z) and transverse (x) directions, at the locations indicated in Figure 1. Penetration ratio (depth over indenter radius) values of around 10–20% were used. Indentation was carried out using a sphere of 1 mm radius, with the indent profiles normally measured using a stylus profilometer. If a sample exhibits in-plane isotropy, then the indent profile will be radially symmetric. However, if there are any in-plane directions that are "softer" than others, this will be apparent in the form of greater pile-up heights for scans made in those directions and possibly a larger indent diameter in that direction. Pile-up height variations constitute a sensitive test for the detection of (in-plane) anisotropy (provided that the material is homogeneous on the scale of the indent, that is, over a distance of the order of a mm). Local inhomogeneity (on a scale of hundreds of micrometers) could give effects similar to those of anisotropy, although this is likely to be detectable in the form of individual scans not being symmetrical about the indentation axis. Such local

inhomogeneity is not common, although it has been observed and investigated recently using PIP to study particulate MMCs.[26]

3. Mechanical Characterization

3.1. Uniaxial Testing

Nominal stress–strain curves from "horizontal" and "vertical" samples in the as-built condition, for both tensile and compressive testing, are shown in **Figure 2**. Indications are also given of the testing directions (relative to the build axis, z) and of the distance of the sample from the build plate. Both pairs of compressive curves are virtually identical, implying that this material is at least approximately isotropic, both close to the build plate and some distance away. On the other hand, the response is significantly different in the two locations (harder close to the plate).

Accurate comparison between tensile and compressive curves is difficult, partly because necking occurs in tension at only about 2% plastic strain, that is, this material shows little work hardening. Postyielding comparison is thus limited. The yield stress in tension is around 1050 MPa for the "horizontal" location (close to the build plate) and about 900 MPa for the "vertical" location (far from the build plate), although yielding is somewhat transitional and these are not accurate figures. However, they are broadly consistent with the compression curves (Figure 2b), although picking up an accurate yield stress from a compression curve is complicated by the effect of friction (which is virtually unavoidable). This tends to raise the value of an apparent yield stress (and subsequent flow stresses), typically by about 5–10%.

Slightly more accurate figures can be obtained for the UTS, which is about 1180 MPa for the "horizontal" location and around 1060 MPa for the "vertical" location. These figures also suggest that material in the former location is about 10% harder than in the latter (remote from the build plate), although for the UTS no direct comparison can be made with the
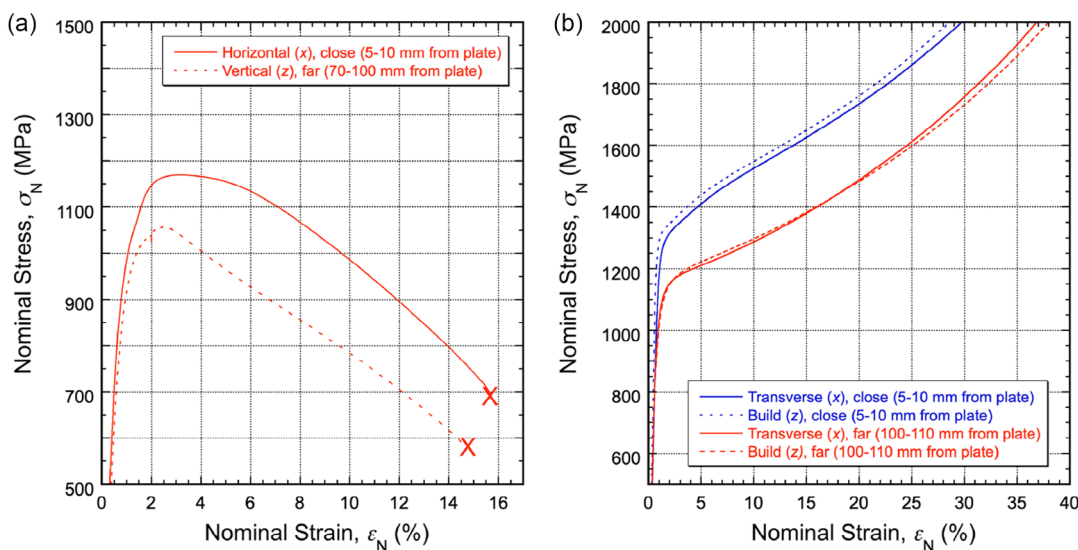
Figure 2. Uniaxial stress–strain curves, for as-built material: a) tensile and b) compressive. Indications are given of the testing directions and the approximate distances from the build plate.

ADVANCED
SCIENCE NEWS
www.advancedsciencenews.com

steel
research
international

www.steel-research.de

compression curves. These tensile test outcomes were previously interpreted[5,16] as indicating that the build direction was softer than the transverse direction. Anisotropy of this type in AM material has been reported previously a number of times, see, for example, the study of Tang et al.[27] However, the compression curves clearly indicate that this difference is not in fact due to anisotropy, but is instead a reflection of the material being softer at greater distances from the build plate.

Corresponding stress–strain curves for the age-hardened material are shown in **Figure 3**. Of course, this material is considerably harder. The two tensile curves again appear to show (relatively small) anisotropy, again with the material close to the plate ("horizontal") being softer, but again the compression data indicate that there is little or no anisotropy. The clear conclusion from these results, is that the differences between the two tensile curves are due, not to the orientation of the test pieces, but to their location (distance from the build plate).

3.2. PIP Testing

PIP testing, in addition to allowing stress–strain curves to be obtained quickly and conveniently, is well suited for exploration of both inhomogeneity (on scales ranging from about a mm to many cm) and anisotropy (assuming that the material is homogeneous on a scale of several hundred micrometers). It is therefore a powerful technique for study of situations like the current one.

3.2.1. Indent Profiles

Indents were made in various locations, and in different directions, on all four types of material, that is, both "horizontal" and "vertical" configurations, for both as-built and age-hardened material. Each indent is given a designation of the form α-β-γ-xx, where α is either A (as-built) or P (precipitation hardened),

β is either H (horizontal) or V (vertical), γ (direction of indentation) is either B (build) or T (transverse), and xx is the approximate distance (in mm) of the indent location from the build plate.
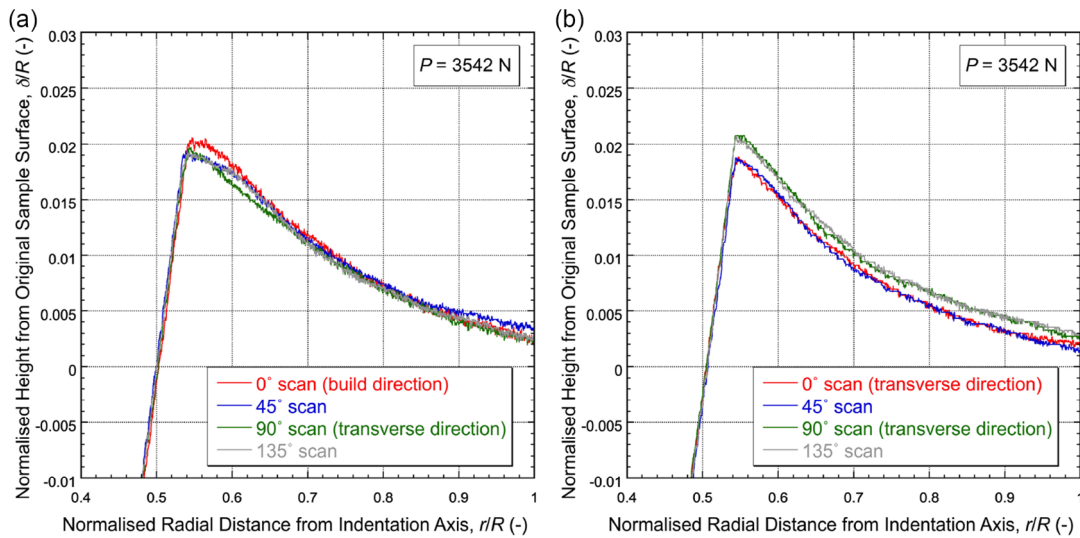
The first issue to check is whether there is in fact significant anisotropy (radial asymmetry in the indent profile) in any location. In-plane (plastic) anisotropy is routinely detectable during PIP testing in the form of differences between pile-up heights for scans in different directions, although it may also be manifested in the form of variations in "indent diameter" in different scan directions. Since the principal axes in these materials are expected to be the B and T directions (with all T directions normal to B being equivalent), indent directions can be limited to these two. The expectation is that all indents in the B direction will exhibit radial symmetry, but indents in a T direction may exhibit asymmetry (if the material is plastically anisotropic).

A typical pair of profile scans (expanded in the pile-up region) is shown in **Figure 4**. These are for as-built material, close to the build plate, with the indentation axis being T (Figure 4a) or B (Figure 4b). These profiles confirm that, at least to a good approximation, both indents are radially symmetric. (The height differences in Figure 4b are around $2\,\mu m$, which is close to the resolution of the profilometer, so these variations are considered to be within experimental error.) A similar pair of scan sets, for the as-built material at greater distances from the build plate, is shown in **Figure 5**. These also exhibit negligible radial symmetry, confirming that the material in this region is also isotropic.
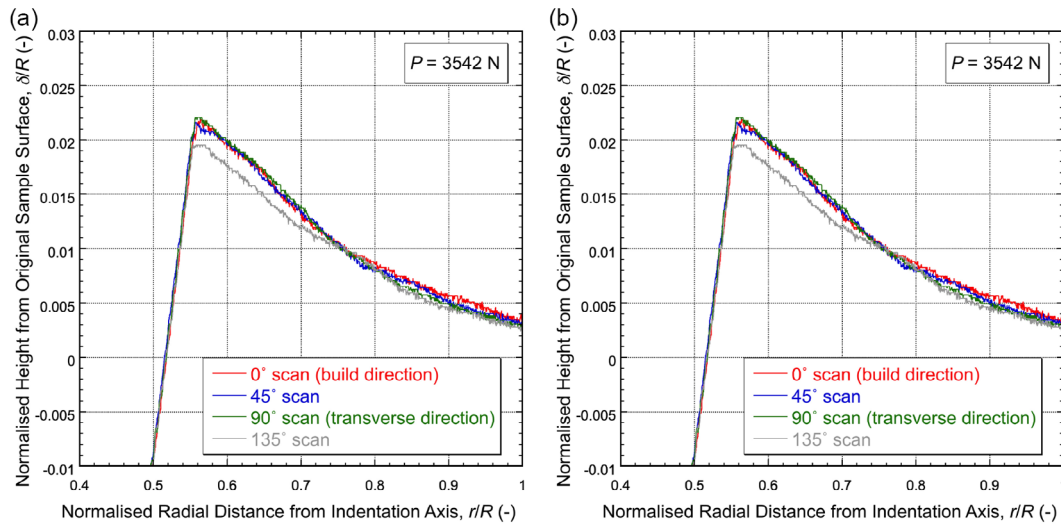
The PIP testing also allows stress–strain curves to be obtained, by converging on the values of the parameters in the V_{oce} law, giving best fit between measured and modeled indent profiles. An example is shown in **Figure 6** of the level of agreement obtained in this work, in this case for the case shown in Figure 4a. As with most PIP testing, use of the optimized stress–strain curve leads to profiles that are in very close agreement with the experimental ones.
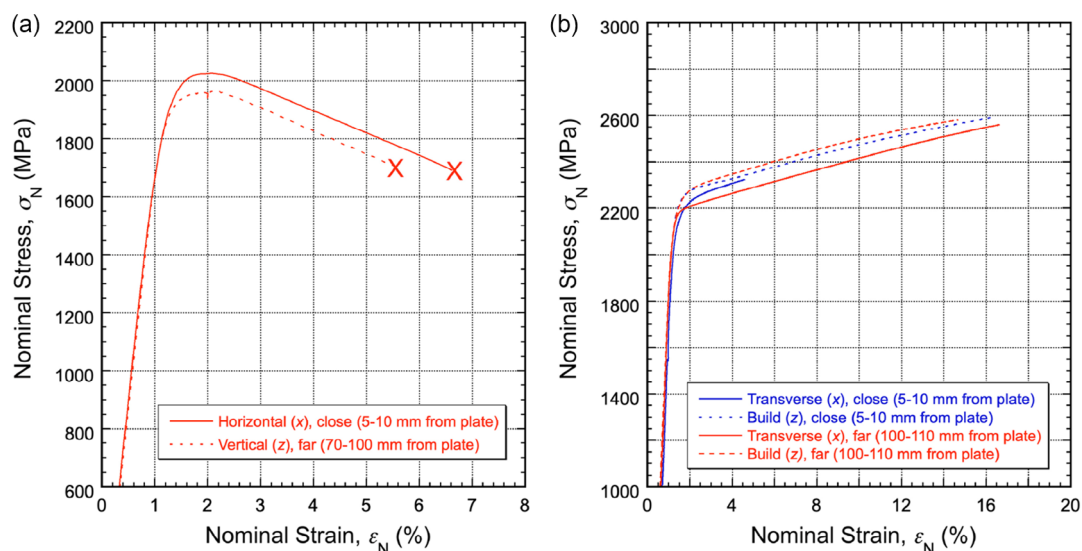
Figure 3. Uniaxial stress–strain curves, for age-hardened material: a) tensile and b) compressive. Indications are given of the testing directions and the approximate distances from the build plate.

**ADVANCED
SCIENCE NEWS**

www.advancedsciencenews.com

**steel
research**
international

www.steel-research.de

Figure 4. Sets of pile-up region scans from indents designated as a) A-H-T-5 and b) A-H-B-5.

**Figure 5.** Sets of pile-up region scans from indents designated as a) A-V-T-60 and b) A-V-T-120.

An obvious question concerns the sensitivity with which (in-plane) anisotropy (if it is indeed present) can be detected via pile-up height differences. This sensitivity has in fact been shown previously[23,27,28] to be high, but it is helpful to give an indication of this in the context of this material. Indents were therefore made into the gauge length of a sample that had been tensile tested, both in the uniformly deformed region and in a location close to the neck, where the plastic strain, while not well defined, was appreciably higher. It might in general be expected that such prior (uniaxial) straining could generate some anisotropy in the material, although it is unlikely to be very strong.

The resultant data are shown in **Figure 7**, which presents profiles in different scan directions for indents in as-built material close to the build plate. The resultant anisotropy is clearly detected, particularly in the neck region, with the tensile

straining direction becoming a little harder, relative to the direction normal to this (which is in fact the build direction). It follows that the absence of significant radial asymmetry in PIP profiles in the as-built and age-hardened samples is a strong indicator of isotropy.

3.2.2. Uniaxial and PIP-Inferred Stress–Strain Curves

A prime objective of PIP testing is to obtain (true) stress–strain curves (from an indent profile) and perhaps to compare these, when converted to nominal plots, with those obtained conventionally via uniaxial testing. Examples are shown in **Figure 8**, which relate to both as-built and age-hardened samples in both horizontal and vertical configurations (i.e., in "near" and "far" locations, relative to the build plate). A couple of general points should first be noted. One is that the PIP curves are only shown
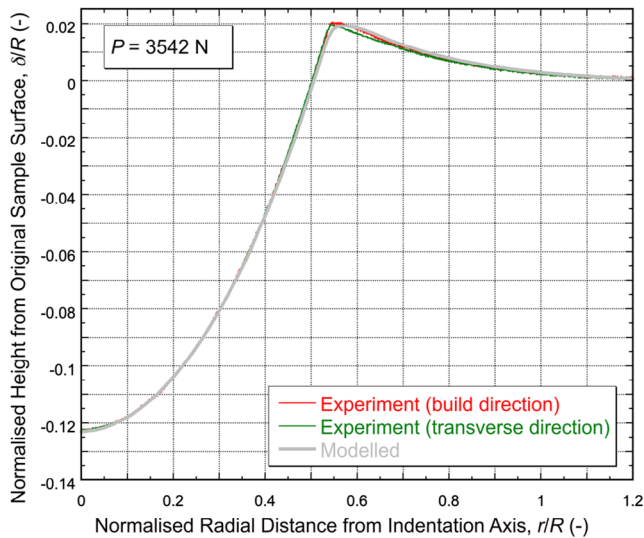
Figure 6. Comparison between measured and modeled profiles for A-H-T-5.

up to the onset of necking, which coincides with the peak in a nominal stress–strain plot. (Prediction of the post-necking regime can be undertaken, but only via FEM modeling, for the specific dimensions of the tensile sample.) Second, the PIP procedure is not sensitive to the exact shape of any transitional yielding in the curve.

Accepting these limitations, good agreement is seen between tensile and PIP test outcomes, for both materials. It follows that the observed "softening", that is, the "vertical" plot being below the "horizontal" one, does not reflect anisotropy in the material, but rather the fact that there is a tendency for the material to become softer at increasing distances from the build plate. This may not be a progressive effect, but material very

close to the build plate, that is, in a "horizontal" sample, is certainly harder than material some distance away, that is, in a "vertical" sample. A further point to note is that, while the same trends are observed for both materials, the difference between the pairs of curves is less for the age-hardened material (Figure 8b). While the difference between the curves for the two orientations (i.e., actually for the two locations) is about 10% for the as-built material, it is only about 3% for the age-hardened material. This is confirmed by both tensile and PIP test outcomes.
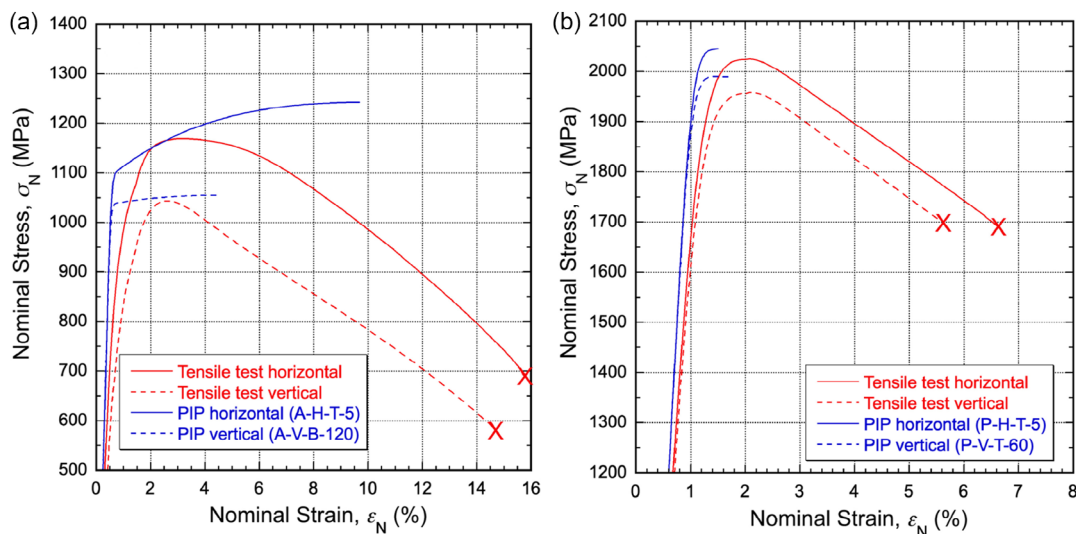
4. Microstructure

4.1. Optical Microscopy

Two low-magnification optical micrographs of regions around indents are shown in **Figure 9**. The main point to note here is that, within experimental error, the indent "diameters" are the same in all directions, that is, these indents are radially symmetric. This is a slightly different indication of isotropy from that of the pile-up heights being the same in all scan directions. It might be expected that this measure would be slightly less susceptible to effects of local inhomogeneities in the microstructure than pile-up height variations. Such a susceptibility is highlighted in a recent paper[26] involving the application of PIP to particulate metal matrix composites, in which there do tend to be local inhomogeneities (relating mainly to particle distributions). On the other hand, pile-up heights can be measured with greater accuracy and are more sensitive to anisotropy (in the absence of local inhomogeneity). Indent diameter measurements (via optical microscopy) are likely to be less sensitive and also potentially affected by focusing effects or any tilting of the sample. In any event, the evidence presented here (from both PIP and compression testing) clearly indicates that this material is isotropic in all locations.
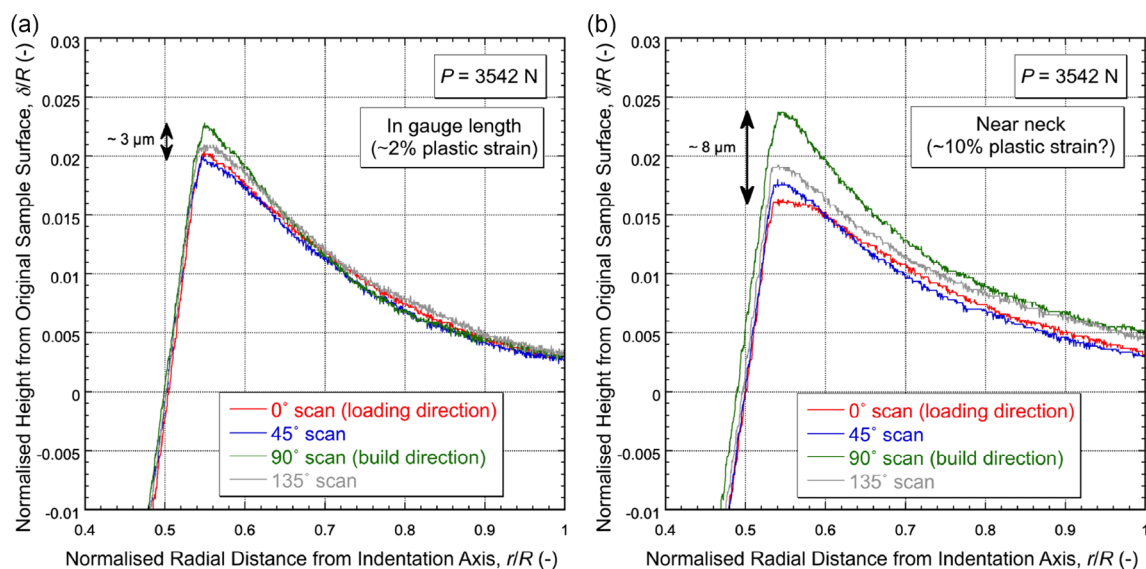
Figure 7. Pile-up region scans from indents in a tensile-tested sample a) in the gauge length and b) in the necked region. Both indent locations would have a designation of A-H-T-5.

2200881 (7 of 10)

ADVANCED
SCIENCE NEWS
www.advancedsciencenews.com

steel
research
international

www.steel-research.de

Figure 8. Comparisons between (nominal) tensile stress–strain curves obtained by conventional uniaxial loading and via PIP testing (for the indent locations and orientations shown), for a) as-built and b) age-hardened material.
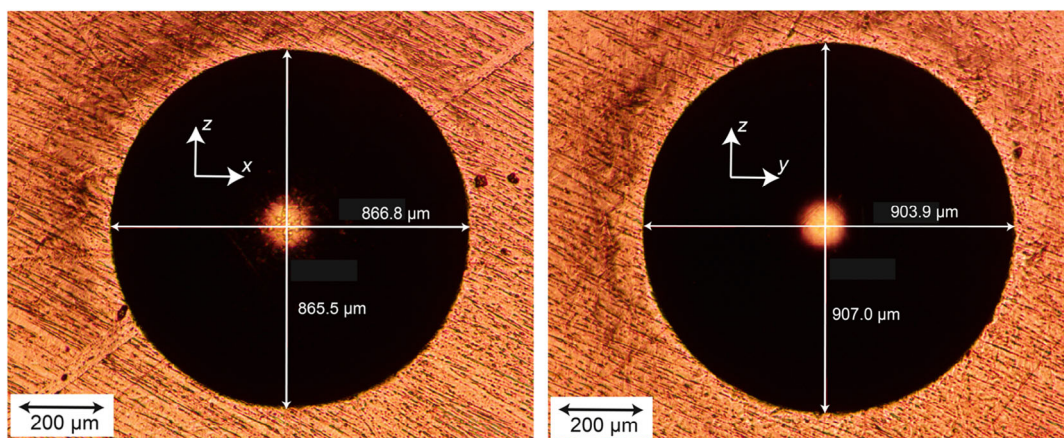
Figure 9. Optical micrographs of indents in two transverse planes of an as-built sample, both designated A-H-T-5, with measured indent diameters. The loads used to create these indents were 1.898 kN (left) and 2.277 kN (right).

### 4.2. SEM Microscopy and Characterization of Texture

Study of EBSD images from various locations, such as those in **Figure 10**, indicated that there was little or no clear texture anywhere. This is consistent with the finding that there appears to be no anisotropy in any of this material. On the other hand, there is a noticeable trend for the grain structure to become a little coarser at greater distances from the build plate. This is not unexpected, since the heat flow and growth conditions are likely to change with distance from the build plate. For example, a decrease in cooling rate is likely. This could lead to (relatively small) differences in mechanical properties in different locations, that is, some progressive inhomogeneity. These micrographs therefore provide further evidence confirming that: 1) there is no anisotropy anywhere in any of this material and 2) there are progressive changes in the material with increasing distance from the build plate, leading to (relatively small) changes in properties, notably a degree of softening.

Finally, it was confirmed that, in the heavily strained region of the neck in the (horizontal) tensile tested sample (where the PIP testing indicated that the material was anisotropic), the material did exhibit noticeable texture. This can be seen from the pole figure shown in **Figure 11**.

5. Conclusion

This study concerns the detection and characterization of anisotropy and inhomogeneity in samples of a maraging steel produced by laser powder bed fusion (with and without subsequent age hardening). The relatively novel technique of PIP has figured extensively in the investigation. The following points have been established. 1) Samples were produced in both "horizontal" and "vertical" configurations, with all of the material being close to the build plate in the former case, while it was much further away (and covered a range of distances from it) in the latter. This was done solely for reasons of experimental
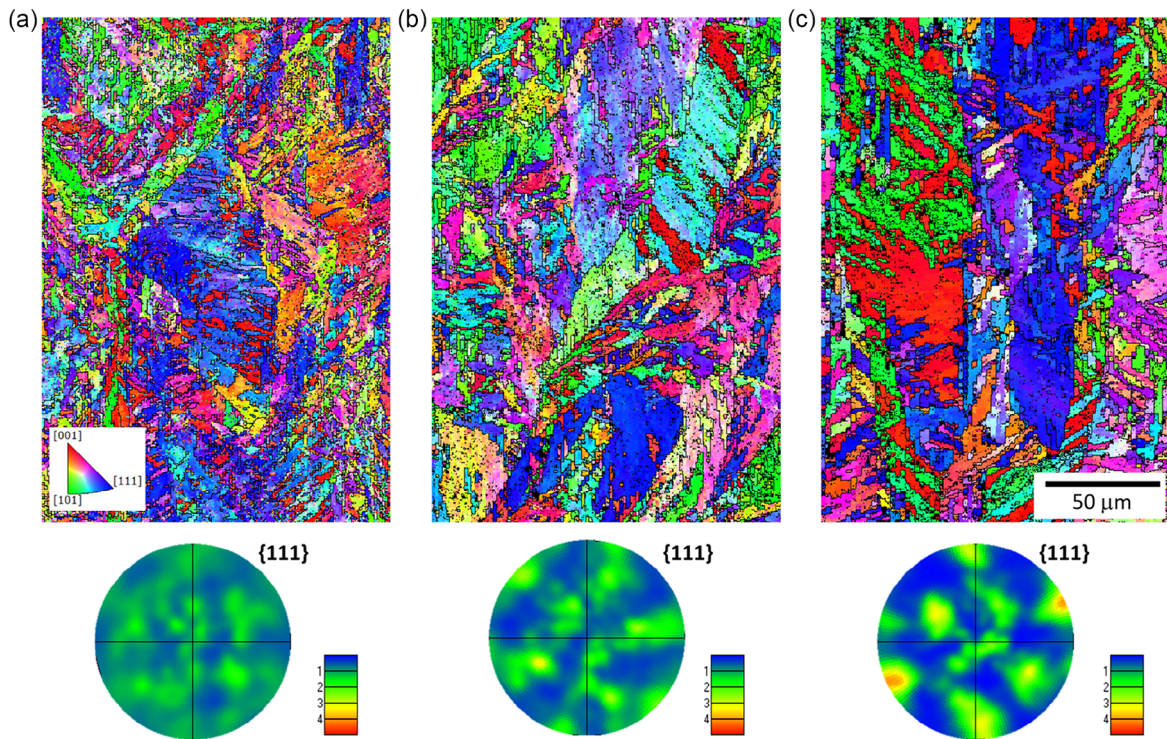
Figure 10. Inverse pole figures along *Y*-axis (upper row) and (111)-type pole figures (lower row) from the as-built material at approximate distances from the build plate of: a) 5 mm, b) 50 mm, and c) 100 mm.
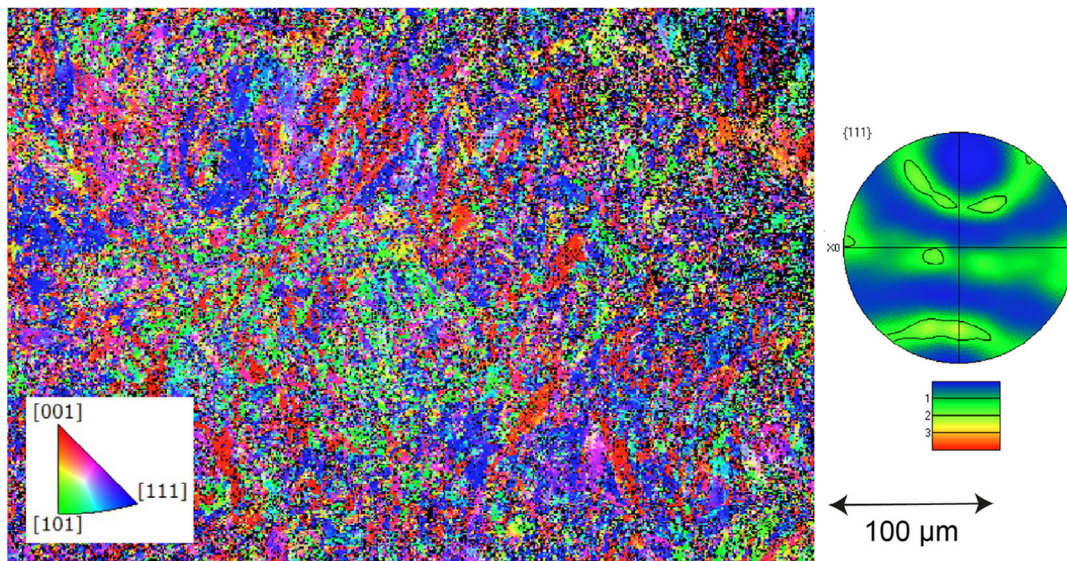
Figure 11. Inverse pole figure along *X*-axis (left) and (111)-type pole figure (right) from the region of the neck in the as-built material after tensile testing.

convenience. Although the material labeled as horizontal was noticeably harder in the tensile test, it is shown here that this was not a consequence of its orientation, but was rather due to it being closer to the build plate. 2) This was confirmed by carrying out compression tests in both "build" and "transverse" directions, at different distances from the build plate. These results indicated that there was little or no anisotropy at any location. Moreover, this result was confirmed by PIP testing, which

has a high sensitivity for the detection of anisotropy (as a lack of radial symmetry in the indent profile). This sensitivity was confirmed for this material via testing of the necked region from a tensile test piece, where the prior plastic strain generated some anisotropy. 3) It is concluded that the apparent anisotropy, as observed in the tensile test, is in fact solely due to inhomogeneity, with a tendency for the material to become a little softer at greater distances from the build plate. This also was confirmed by both

compression testing and PIP testing. It applies to both as-built and age-hardened material, although the effect is weaker in the latter. 4) These conclusions are supported by microstructural evidence, with EBSD data indicating that the material is untextured in all locations, but with a tendency for the grain size to be larger at greater distances from the build plate. Furthermore, some texture was exhibited by material from the necked region of a tensile test piece, in which anisotropy was detected.

Conflict of Interest

The authors declare no conflict of interest.

Data Availability Statement

The data that support the findings of this study are available from the corresponding author upon reasonable request.

[1] X. F. Xu, S. Ganguly, J. L. Ding, S. Guo, S. William, F. Martina, *Mater. Charact.* **2018**, *143*, 152.

[2] X. F. Xu, J. L. Ding, S. Ganguly, C. L. Diao, S. Williams, *J. Mater. Eng. Perform.* **2019**, *28*, 594.

[3] K. Pancikiewicz, *Materials* **2021**, *14*, 6725.

[4] S. Shakerin, A. Hadadzadeh, B. S. Amirkhiz, S. Shamsdini, J. Li, M. Mohammadi, *Addit. Manuf.* **2019**, *29*, 100797.

[5] B. Mooney, K. I. Kourousis, R. Raghavendra, D. Agius, *Mater. Sci. Eng., A* **2019**, *745*, 115.

[6] L. Kucerova, I. Zetkova, A. Jandova, M. Bystriansk, *Mater. Sci. Eng., A* **2019**, *750*, 70.

[7] A. Hadadzadeh, A. Shahriari, B. S. Amirkhiz, J. Li, M. Mohammadi, *Mater. Sci. Eng., A* **2020**, *787*, 139470.

[8] B. Mooney, K. I. Kourousis, *Metals* **2020**, *10*, 1273.

[9] A. E. W. Jarfors, T. Matsushita, D. Siafakas, R. Stolt, *Mater. Des.* **2021**, *204*, 109608.

[10] Z. Brytan, M. Krol, M. Benedyk, W. Pakiela, T. Tanski, M. J. Dagnaw, P. Snopinski, M. Pagac, A. Czech, *Materials* **2022**, *15*, 1734.

[11] J. E. Campbell, M. Gaiser-Porter, W. Gu, S. Ooi, M. Burley, J. Dean, T. W. Clyne, *Adv. Eng. Mater.* **2022**, *24*, 2101398.

[12] V. A. Popovich, E. V. Borisov, A. A. Popovich, V. S. Sufiiarov, D. V. Masaylo, L. Alzina, *Mater. Des.* **2017**, *114*, 441.

[13] K. Chang, X. Wang, E. Q. Liang, R. Zhang, *Vacuum* **2020**, *181*, 109732.

[14] D. Barba, C. Alabort, Y. T. Tang, M. J. Viscasillas, R. C. Reed, E. Alabort, *Mater. Des.* **2020**, *186*, 108235.

[15] K. Hagihara, T. Nakano, *JOM* **2022**, *74*, 1760.

[16] B. Mooney, K. I. Kourousis, R. Raghavendra, *Addit. Manuf.* **2019**, *25*, 19.

[17] Z. J. Zhao, L. Wang, D. C. Kong, P. F. Liu, X. He, X. Q. Ni, L. Zhang, C. F. Dong, *Mater. Charact.* **2022**, *189*, 111938.

[18] E. W. Hovig, A. S. Azar, K. Solberg, K. Sorby, *Int. J. Adv. Manuf. Technol.* **2021**, *114*, 1359.

[19] Y. Tian, K. Nyamuchiwa, K. Chadha, Y. L. He, C. Aranas, *Mater. Sci. Eng., A* **2022**, *839*, 142827.

[20] R. Kannan, P. Nandwana, *Sci. Rep.* **2022**, *12*, https://doi.org/10.1038/s41598-022-09977-1.

[21] M. J. Paul, Y. Muniandy, J. J. Kruzic, U. Ramamurty, B. Gludovatz, *Mat. Sci. Eng., A* **2022**, *844*, 143167.

[22] S. Dehgahi, M. Sanjari, M. H. Ghoncheh, B. S. Amirkhiz, M. Mohammadi, *Addit. Manuf.* **2021**, *39*, 101847.

[23] T. W. Clyne, J. E. Campbell, M. Burley, J. Dean, *Adv. Eng. Mater.* **2021**, *23*, 2100437.

[24] M. Burley, J. E. Campbell, R. Reiff-Musgrove, J. Dean, T. W. Clyne, *Adv. Eng. Mater.* **2021**, *23*, 2001478.

[25] W. Gu, J. E. Campbell, Y. T. Tang, H. Safaie, R. Johnston, Y. Gu, C. Pleydell-Pearce, M. Burley, J. Dean, T. W. Clyne, *Adv. Eng. Mater.* **2022**, *24*, 2101645.

[26] R. Reiff-Musgrove, M. Gaiser-Porter, W. Gu, J. E. Campbell, P. Lewis, A. Frehn, A. D. Tarrant, Y. T. Tang, M. Burley, T. W. Clyne, *Adv. Eng. Mater.* **2023**, *2201479*, https://doi.org/10.1002/adem.202201479.

[27] Y. T. Tang, J. E. Campbell, M. Burley, J. Dean, R. C. Reed, T. W. Clyne, *Materialia* **2021**, *15*, https://doi.org/10.2139/ssrn.3746800.

[28] Y. T. Tang, R. Reiff-Musgrove, W. Gu, J. E. Campbell, M. Burley, J. Dean, T. W. Clyne, *Mat. Sci. Eng., A* **2022**, *848*, 143429.